DOI: https://doi.org/10.37434/tpwj2023.08.05

INFLUENCE OF WELD POOL SURFACE DEPRESSION ON BURNING CONDITIONS OF AN ARC WITH A REFRACTORY CATHODE

I.V. Krivtsun, I.V. Krikent, V.F. Demchenko

E.O. Paton Electric Welding Institute of the NASU
11 Kazymyr Malevych Str., 03150, Kyiv, Ukraine

ABSTRACT

Results of mathematical modeling of an argon arc with refractory cathode in case of a deformed surface of the weld pool (arc anode) are described. It is assumed that there is a depression (crater) on the anode surface, the shape and size of which are preset; arc plasma has axial symmetry, and it is in a stationary state; metal evaporation from the anode surface is ignored. A mathematical model of the processes of energy, momentum, mass and charge transfer in the arc column and anode region is briefly described. A numerical study was conducted of thermal, electromagnetic and gas-dynamic processes in the arc column with a curved surface of the anode, as well as conditions of electric, thermal and force interaction of the arc with the anode surface, depending on the crater depth. Results of computational experiments are illustrated by the fields of isotherms, isobars and current lines in an arc with a curved surface of the anode, which are compared with similar fields in the case of an anode with a plane surface. A procedure for calculation of normal components of the vectors of electric current density and specific heat flux into the anode with a curved surface is described, and results of calculation of radial distributions of these characteristics, depending on the depth of the crater on the anode surface, are given. These results are complemented by numerical studies of the influence of the crater depth on arc pressure distribution over the anode surface. A conclusion was made that sagging of the weld pool surface in TIG welding can significantly change the conditions of electric and thermal interaction of the arc with the metal being welded, namely it can influence the thermal and hydrodynamic processes in the liquid metal, which determine the penetrability of the arc with the refractory cathode.

KEYWORDS: TIG welding, arc column, anode region, weld pool surface, anode, electric current density, specific heat flux into the anode, mathematical modeling

INTRODUCTION

Technological results of TIG welding are largely determined by the conditions of electric arc interaction with the surface of the metal being welded. Such conditions include: distributions of the specific heat flux, electric current density, gas-dynamic pressure and stress of viscous friction of arc plasma on the weld pool surface. In their turn, these conditions determine the thermal, electromagnetic and hydrodynamic processes in the metal being welded, and the depth and shape of its penetration, respectively.

A large number of studies are devoted to investigations of plasma column and anode region of an electric arc with a refractory cathode, including the conditions of its interaction with the anode surface, depending on current, arc length, cathode shape and dimensions, shielding gas composition and pressure [1–14]. Experimental studies of the distributions of electric current density and specific heat flux over the anode surface in [1, 6, 10] were conducted using the method of split water-cooled anode with a plane working surface. A water-cooled anode with a plane surface was also used during spectrometric measurements of arc plasma temperature in [3, 7] and probe measurements of electron temperature and plasma potential in the arc anode region [5]. Theoretical studies and numerical modeling of the processes in the column and anode boundary layer of an arc with a refractory cathode, performed in [2–4, 7–9, 11–14], were conducted with the assumption that the anode surface temperature is not higher than its material melting temperature, and the surface proper is plane. The thus obtained results do not allow fully taking into account the influence of weld pool surface deformation and its temperature on the thermal, gas-dynamic and electromagnetic characteristics of arc plasma, as well as on the processes in the metal being welded by a nonconsumable electrode arc.

Works [15–21] are devoted to studying the influence of the anode surface temperature on the abovementioned characteristics, in particular on its material evaporation into arc plasma. In the majority of such theoretical works (see, for instance, reviews [17, 18] and references cited in them) the surface of the anode (weld pool) is also considered to be plane, and distribution of this surface temperature either is found by calculation using various models of the processes running in the anode body [15–19], or it is assigned *a priori* [20, 21].

Under the conditions of TIG welding, the pressure of arc plasma on the surface of the material be-

ing welded can considerably (depending on current and arc length) deform the melt surface. In this case, distribution of normal components of electric current density and specific heat flux into the anode, as well as distribution of gas-dynamic pressure of arc plasma along the weld pool surface can differ essentially from those determined during full-scale or numerical experiments for an anode with a plane surface. Eventually, it may lead to a change in the thermal or hydrodynamic situation in liquid metal and, consequently, it can influence the arc penetrability in TIG welding.

The works devoted to modeling the physical processes in welding by a constricted (plasma) arc and free-burning arc, with allowing for deformation of the weld pool free surface, appeared recently [22–24]. In these studies a unified mathematical model is used to describe a set of physical processes running in the arc column and anode region, as well as processes in the metal being welded. Such an approach allowed modeling the process of spot TIG welding at high values of arc current [23], i.e. under the conditions, when weld pool surface deformation turns out to be considerable, and studying the processes of plasma welding in the keyhole penetration mode in spot [22] and linear [24] plasma-arc welding. At the same time, the unified mathematical model used by the authors of [22–24], does not allow fully taking into account the specifics of the anode processes, which in the abovementioned works, were described using a diffusion approximation for the anode boundary layer plasma, which is assumed to be isothermal (local-thermal-equilibrium approximation) [25].

Thus, this work is devoted to computer modeling of the processes of transfer of energy, momentum, mass and charge in the plasma of the arc column and anode region of atmospheric pressure argon arc with a refractory cathode and an anode with a curved surface, based on a self-consistent mathematical model, which was proposed in [11, 12], used and verified in [13]. A computational experiment is used to study both the distributed characteristics of arc plasma, and the conditions of its interaction with the curved surface of the anode.

CONDITIONS OF COMPUTATIONAL EXPERIMENT

The most adequate description of the process of TIG welding allowing for deformation of the weld pool surface, should be based on a conjugated model, which describes the thermal, electromagnetic and gas/hydrodynamic processes in "arc plasma–anode boundary layer–metal being welded" system. Computer realization of such a model involves considerable difficulties, and it requires significant computing resources. In this work an approximate approach is used to study the influence of weld pool surface deformation on the conditions of burning of an argon arc with a refractory cathode. This approach is based on the following postulates:

1. The deformed surface of the weld pool is approximated by axially symmetric depression on the anode surface. The shape of this depression (crater) is assumed to be unchanged in time and *a priori* assigned as a surface of revolution with the generatrix described by the following equation $z = ar^2$. In this formula, z coordinate is calculated from the crater bottom; $a = L/R^2$; where L, R are the depth and radius of the crater (Figure 1).

2. It is assumed that the processes of transfer of energy, momentum, mass and charge in the arc discharge are stationary, and distributions of arc plasma characteristics are axially symmetric.

3. The processes of energy, momentum, mass and charge transfer in the boundary arc column and anode layer are described using a self-consistent mathematical model [11–13], which includes two interrelated models:

- arc column model, describing the thermal, electromagnetic, and gas-dynamic processes in the arc column plasma, which is assumed to be quasineutral, isothermal and ionisationally equilibrium;
- anode boundary layer model, which describes the processes in near-anode plasma, allowing for its thermal and ionisational non-equilibrium, as well as presence near the anode surface of a space charge layer, and which allows formulation of boundary conditions on the interface of arc column plasma with the anode region and calculation of distributed character-

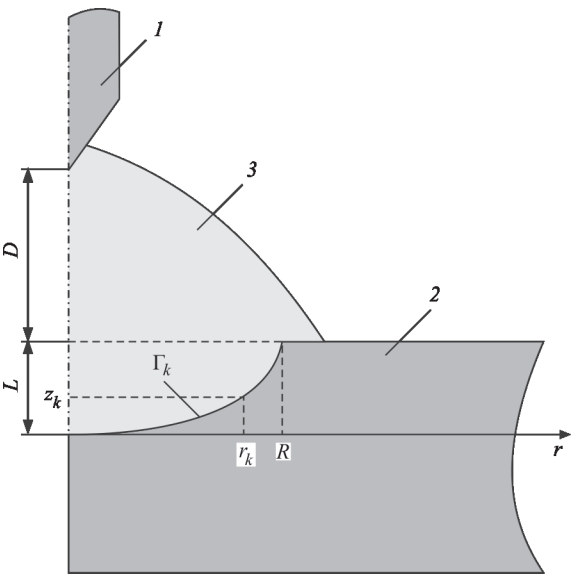

Figure 1. Schematic representation of arc-anode system: *1* — refractory cathode; *2* — anode; *3* — arc

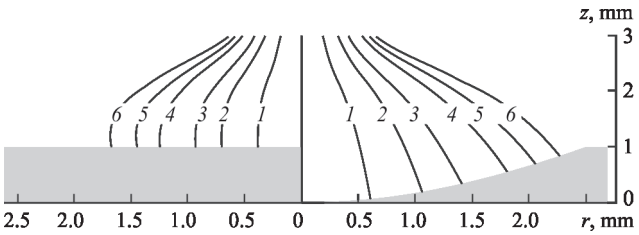

Figure 2. Current lines in arc column: *1* — i = 10; *2* — 30; *3* — 50; *4* — 80; *5* — 100; *6* — 120 A

istics of thermal, gas-dynamic and electromagnetic interaction of arc plasma with the anode surface.

4. Metal evaporation from the anode surface is not taken into account, which is valid, for instance, for a steel anode, if the maximum temperature of its surface does not exceed 2400 K [20].

Numerical realization of the mathematical model [11, 12] was performed on a rectangular mesh by finite difference method, using a compatible Lagrangian–Eulerian technique [26], adapted to the conditions of a compressive medium. In the mesh area the boundary between the plasma and metal was approximated by a stepped line. An argon arc of length D = 2 mm (distance from the cathode to uncurved surface of the anode, see Figure 1) at current I = 200 A was considered. Calculated data from [27, 28] were used to determine the thermodynamic and transport properties, as well as energy losses for radiation of atmospheric pressure argon plasma, depending on temperature.

During mathematical modeling the distributions of thermal, electromagnetic and gas-dynamic characteristics of plasma in the arc column were calculated, as well as distributed characteristics of arc interaction with anode surface, depending on the depth of the crater on this surface. During performance of calculation experiments R = 2.5 mm was assumed, and L value was varied in the range of 0–1.4 mm.

MODELING RESULTS

We will select L = 1 mm as a characteristic value of crater depth on the anode surface, and will see how the curvature of the anode surface influences the electromagnetic, thermal and gas-dynamic processes in arc plasma. Figures 2–4 shows the current lines, isotherms and isobars of excess pressure Δp in arc column plasma, calculated for a plane (on the left in the Figure) and curved (on the right in the Figure) surface of the anode. The current lines are understood to be the generatrices of the surfaces of revolution, which limit the arc plasma regions, through which the set fraction i of full arc current I flows.

The curved surface of the anode essentially changes the mode of current passage and the thermal and gas-dynamic situation in the arc column. Surface sagging has the greatest influence on the characteristics of the arc discharge near the anode, and it is still manifested in the middle of the interelectrode gap. In the near-cathode region the arc characteristics differ slightly from the case of an anode with a plane surface. This conclusion, which follows from analysis of the fields in Figures 2–4, is supported by the results of calculation of current density in two cross-sections of the arc column: in the plane of an uncurved surface of the anode (Figure 5, *a*); and in the plane located above this surface at 0.5 mm distance (Figure 5, *b*).

We will determine the distributions of normal components of the vectors of electric current density j_{an} and specific heat flux q_{an} on the curved surface of the anode, which are required at modeling of the thermal, gas-dynamic and electromagnetic processes in the metal being welded, allowing for deformation of the weld pool free surface. At numerical calculation, the vectors of current density and specific heat flux into the anode along the stepped mesh boundary, which approximates the curved surface of the anode Γ, have components both in the axial and in the radial directions (axial components on the horizontal lines of the mesh, and radial components on the vertical lines). This complicates calculation of the respective vector components, normal to the abovementioned surface.

We will use the following procedure to determine j_{an} and q_{an} distributions on the curved surface of the anode. Let Γ_k be a segment of the generatrix of crater surface, which begins from its bottom and ends with a point with coordinates $\{r_k, z_k\}$ on generatrix Γ of the crater (see Figure 1). We will denote as $I_a(r_k) = 2\pi\int_{\tilde{A}_k} j_{an}(s)r(s)ds$ the electric current flowing into the plasma through part of the curvilinear surface of the anode with generatrix Γ_k, and, accordingly, as $Q_a(r_k) = 2\pi\int_{\tilde{A}_k} q_{an}(s)r(s)ds$ the heat flux, which enters

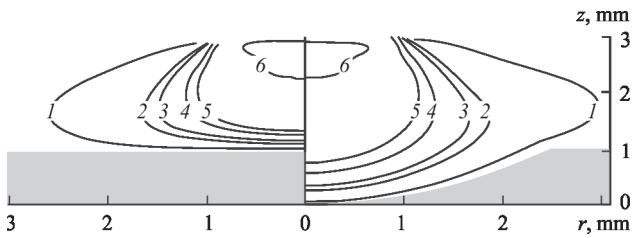

Figure 3. Temperature field of arc column plasma: *1* — T = 13; *2* — 17; *3* — 18; *4* — 20; *5* — 21; *6* — 25 K

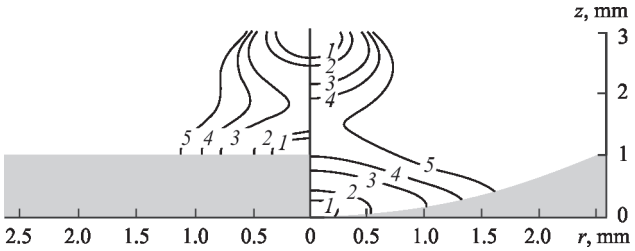

Figure 4. Field of isobars of excess pressure in arc column: *1* — Δp = 800; *2* — 700; *3* — 500; *4* — 400; *5* — 300 Pa

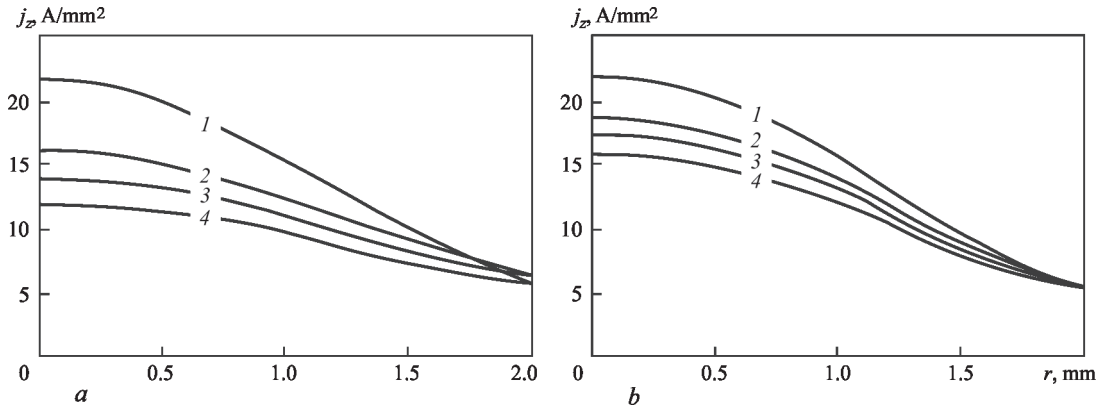

Figure 5. Radial distribution of axial component of current density in two cross cross-sections of arc column at different L values: *1* — L = 0; *2* — 0.7; *3* — 1.0; *4* — 1.4 mm

the anode through the abovementioned surface, where s is the current length of the generatrix Γ.

We will approximately assure:

$$j_{an}(r_k) \approx [(\tilde{I}_a(r_{k+1}) - \tilde{I}_a(r_k)]) / S_k; \quad (1)$$

$$q_{an}(r_k) \approx [(\tilde{Q}_a(r_{k+1}) - \tilde{Q}_a(r_k)]) / S_k, \quad (2)$$

where $j_{an}(r_k)$, $q_{an}(r_k)$ are the mean values of normal to the anode curved surface components of current density and specific heat flow in segment $\Delta\Gamma_k$ of the generatrix between crater sections $z = z_{k+1}$ and $z = z_k$; $S_k = 2\pi\oint_{\Delta\Gamma_k} r(s)ds$ is the surface area of the body of revolution with generatrix $\Delta\Gamma_k$, and $\tilde{I}_a(r_k)$ and $\tilde{Q}_a(r_k)$ are the summing analogs of $I_a(r_r)$ and $Q_a(r_r)$ distributions, respectively.

$\tilde{I}_a(r_k)$, $\tilde{I}_a(r_k)$ were calculated by numerical integration of discrete values of electric current density and specific heat flow along all (both horizontal and vertical) segments of broken mesh boundary Γ_k. Note that at numerical solution of the model equations on a rectangular mesh the mesh values of current and heat flow which are determined along the broken mesh boundary, develop small oscillations. In order to eliminate them, mesh functions $\tilde{I}_a(r_k)$, $\tilde{Q}_a(r_k)$ in

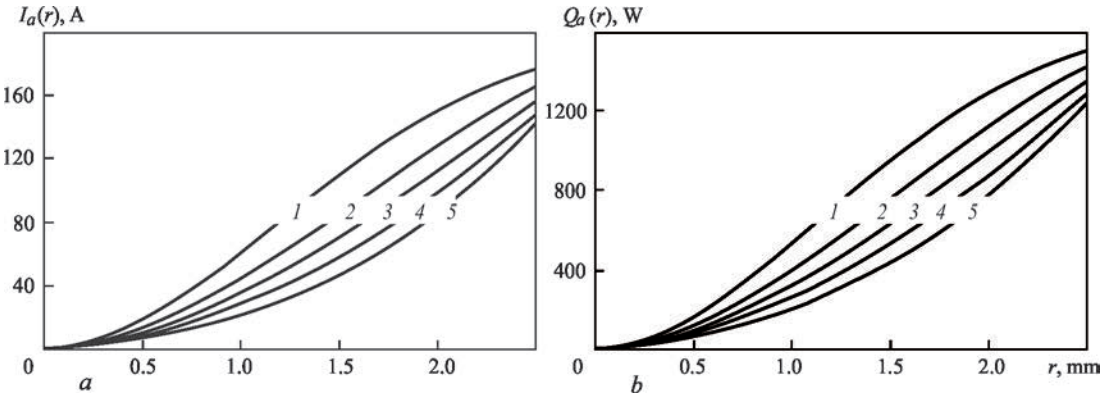

Figure 6. Radial distributions of electric current (*a*) and heat flux through the curved surface of the anode: *1* — L = 0; *2* — 0.4; *3* — 0.7; *4* — 1.0; *5* — 1.4 mm

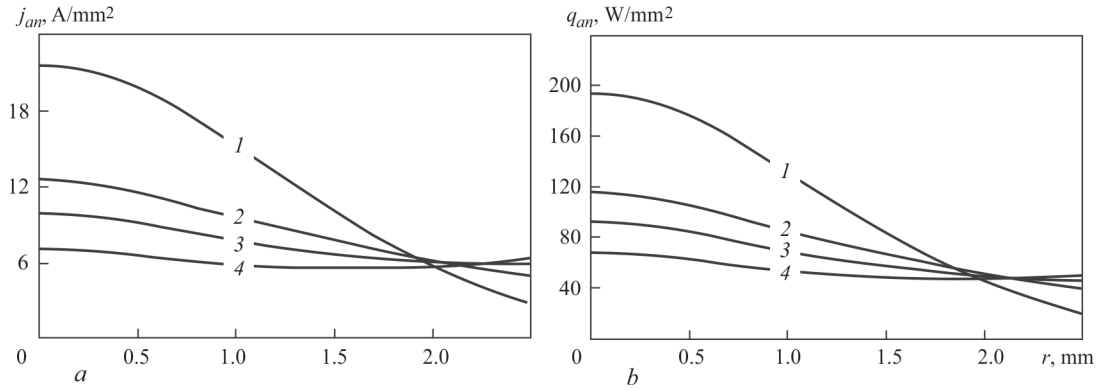

Figure 7. Radial distributions of normal components of vectors of current density (*a*) and specific heat flux (*b*) on anode surface: *1* — L = 0; *2* — 0.7; *3* — 1.0; *4* — 1.4 mm

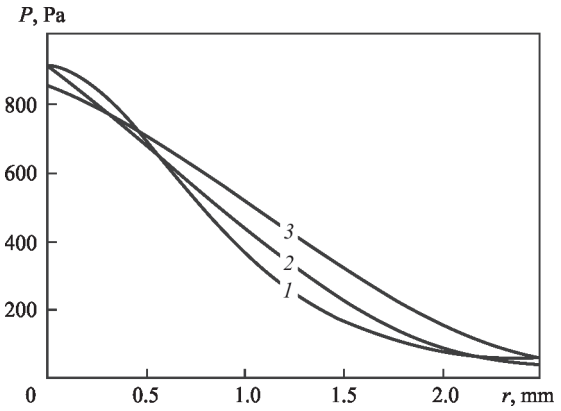

Figure 8. Arc plasma pressure on the curved surface of the anode: *1* — L = 0; *2* — 0.4; *3* — 1.0 mm

$0 \le r \le 2.5$ mm segment are approximated by 3rd order polynomials, and the derived interpolation dependencies are used in (1), (2) at calculation of normal components of electric current density and specific heat flux on the curved surface of the anode.

The thus calculated radial distributions of $I_a(r)$ and $Q_a(r)$ values in the crater on the anode surface are shown in Figure 6. Respective distributions of $j_{an}(r)$, $q_{an}(r)$ for an argon arc with a refractory cathode and an anode with a deformed surface are shown in Figure 7.

With greater sagging of the crater, the area of the anode surface interacting with arc plasma becomes greater. As a result, both these parameters, which are responsible for the electric and thermal interaction of the arc with the anode having a curved surface, decrease with increase of this surface sag. The nature of their distribution along the anode surface also changes.

Unlike the density of anode current and specific heat flow into the anode (see Figure 7), pressure distribution along the curved surface of the anode only slightly depends on the value of its surface sagging (Figure 8). It should be noted that the gas-dynamic pressure, calculated by the method of mathematical modeling is excessive, compared to atmospheric pressure, and it includes two components: magnetic pressure and pressure of arc plasma velocity head, which results from the impact of a non-potential component of the Lorentz force [29].

CONCLUSIONS

In straight polarity TIG welding:

1. Influence of weld pool surface deformation on the thermal, electric and gas-dynamic characteristics of arc plasma is the most pronounced in that part of the arc column, which is removed from the welded metal surface plane to a distance, which is comparable with the value of weld pool sag, and it becomes weaker when moving closer to the cathode.

2. Deformation of weld pool free surface may lead to an essential change of the conditions of thermal, electric and dynamic interaction of the arc with the metal being welded, compared to the case, when the pool surface is plane. Depending on the value of pool surface sag, the axial values of normal components of electric current density and specific heat flux of the arc on the weld pool surface can decrease two times and more. The pressure, applied by the arc plasma flow to the weld pool surface, little depends on the extent of its surface deformation.

3. Influence of pool surface deformation on the arc penetrability consists not only in the heat source moving deeper into the metal being welded, but also in a radical change of the hydrodynamic flows in the weld pool, compared to those predicted by the models, which ignore the weld pool sagging. At pool surface deformation the characteristics of the electromagnetic field in the metal being welded undergo significant changes. These characteristics determine the value and distribution of the Lorentz force as an important force factor influencing the hydrodynamic processes in the weld pool and convective heat transfer in the molten metal.

REFERENCES

1. Nestor, O.H. (1962) Heat intensity and current density distributions at the anode of high current, inert gas arcs. *J. Appl. Phys*., 33(**5**), 1638–1648. DOI: https://doi.org/10.1063/1.1728803
2. Dinulescu, H.A., Pfender, E. (1980) Analysis of the anode boundary layer of high intensity arcs. *J. Appl. Phys*., 51(**6**), 3149–3157. DOI: https://doi.org/10.1063/1.328063
3. Hsu, K.C., Etemadi, K., Pfender, E. (1983) Study of the free-burning high-intensity argon arc. *J. Appl. Phys*., 54(**3**), 1293–1301. DOI: https://doi.org/10.1063/1.332195
4. Hsu, K.C., Pfender, E. (1983) Two-temperature modeling of the free-burning high-intensity arc. *J. Appl. Phys*., 54(**8**), 4359–4366. DOI: https://doi.org/10.1063/1.332672
5. Sanders, N.A., Pfender, E. (1984) Measurement of anode falls and anode heat transfer in atmospheric pressure high intensity arcs. *J. Appl. Phys*., 55(**3**), 714–722. DOI: https://doi.org/10.1063/1.333129
6. Tsai, N.S., Eagar, T.W. (1985) Distribution of the heat and current fluxes in gas tungsten arcs. *Metall. Transact. B*, **16**, 841–846. DOI: https://doi.org/10.1007/BF02667521
7. Schmidt, H.P., Speckhofer, G. (1996) Experimental and theoretical investigation of high-pressure arcs. Pt I: The cylindrical arc column (two-dimensional modelling). *IEEE Transact. Plasma Sci*., 24(**4**), 1229–1238. DOI: https://doi.org/10.1109/27.536570
8. Jenista, J., Heberlein, J.V.R. Pfender, E. (1997) Numerical model of the anode region of high-current electric arcs. *IEEE Transact. Plasma Sci*., 25(**5**), 883–890. DOI: https://doi.org/10.1109/27.649585
9. Goodarzi, M., Choo, R., Toguri, J.M. (1997) The effect of the cathode tip angle on the GTAW arc and weld pool: I. Mathematical model of the arc. *J. Phys. D: Appl. Phys.*, **30**, 2744–2756. DOI: https://doi.org/10.1088/0022-3727/30/19/013
10. Füssel, U., Schnick, M., Munoz, J.E.F. et al. (2007) Experimentelle möglichkeiten der WSG-lichtbogenanalyse. *Schweißen und Schneiden*, 59(**7–8**), 396–403.
11. Krivtsun, I., Demchenko, V., Lesnoi, A. et al. (2009) Model of heat-, mass- and charge-transfer in welding arc column and

anode region. In: *Proc. of the 9th Int. Seminar on Numerical Analysis of Weldability, Graz-Seggau, Austria, 2009*.
12. Krivtsun, I.V., Demchenko, V.F., Krikent, I.V. (2010) Model of the processes of heat-, mass- and charge transfer in the anode region and column of the welding arc with refractory cathode. *The Paton Welding J.*, **6**, 2–9.
13. Krivtsun, I.V., Krikent, I.V., Demchenko, V.F. (2012) Modelling of processes of heat-, mass- and electric transfer in column and anode region of arc with refractory cathode. *The Paton Welding J.*, **3**, 2–6.
14. Semenov, I.L., Krivtsun, I.V., Reisgen, U. (2016) Numerical study of the anode boundary layer in atmospheric pressure arc discharges. *J. Phys. D: Appl. Phys*., **49**, 105204. DOI: https://doi.org/10.1088/0022-3727/49/10/105204
15. Lago, F., Gonzalez, J.J., Freton, P., Gleizes, A. (2004) A numerical modelling of an electric arc and its interaction with the anode: Pt. I: The two-dimensional model. *J. Phys. D: Appl. Phys*., **37**, 883–897. DOI: https://doi.org/10.1088/0022-3727/37/6/013
16. Yamamoto, K., Tanaka, M., Tashiro, S. et al. (2008) Metal vapour behaviour in gas tungsten arc thermal plasma during welding. *Sci. Technol. of Weld. Joining*, 13(**6**), 566–572. DOI: https://doi.org/10.1179/174329308X319235
17. Murphy, A.B., Tanaka, M., Yamamoto, K. et al. (2009) Modelling of thermal plasmas for arc welding: the role of the shielding gas properties and of metal vapour. *J. Phys. D: Appl. Phys*., **42**, 194006. DOI: https://doi.org/10.1088/0022-3727/42/19/194006
18. Murphy, A.B. (2010) The effect of metal vapour in arc welding. *J. Phys. D: Appl. Phys*., **43**, 434001. DOI: https://doi.org/10.1088/0022-3727/43/43/434001
19. Mougenot, J., Gonzalez, J.J., Freton, P., Masquere, M. (2013) Plasma-weld pool interaction in tungsten inert-gas configuration. *J. Phys. D: Appl. Phys*., **46**, 135206. DOI: https://doi.org/10.1088/0022-3727/46/13/135206
20. Krikent, I.V., Krivtsun, I.V., Demchenko, V.F. (2014) Simulation of electric arc with refractory cathode and evaporating anode. *The Paton Welding J.*, **9**, 17–24. DOI: https://doi.org/10.15407/tpwj2014.09.02
21. Krivtsun, I.V., Demchenko, V.F., Krikent, I.V. et al. (2019) Effect of current and arc length on characteristics of arc discharge in nonconsumable electrode welding. *The Paton Welding J.*, **5**, 2–12. DOI: https://doi.org/10.15407/tpwj2019.05.01
22. Jian, X., Wu, C.S. (2015) Numerical analysis of the coupled arc-weld pool-keyhole behaviors in stationary plasma welding. *Int. J. Heat Mass Transfer*, **84**, 839–847. DOI: https://doi.org/10.1016/j.ijheatmasstransfer.2015.01.069
23. Wang, X., Luo, Y., Fan, D. (2019) Investigation of heat and fluid flow in high current GTA welding by a unified model. *Int. J. Therm. Sci*., **142**, 20–29. DOI: https://doi.org/10.1016/j.ijthermalsci.2019.04.005
24. Li, Y., Su, Ch., Wang, L., Wu Ch. (2020) A convenient unified model to display the mobile keyhole-mode arc welding process. *Appl. Sci.*, **10**, 7955. DOI: https://doi.org/10.3390/app10227955
25. Lowke, J.J., Tanaka, M. (2006) LTE-diffusion approximation for arc calculations. *J. Phys. D: Appl. Phys*., **39**, 3634–3643. DOI: https://doi.org/10.1088/0022-3727/39/16/017
26. Demchenko, V., Lesnoi, A. (2000) Lagrange-Euler method of numerical solutions of multidimensional problems of convective diffusion. *Reports of the National Academy of Sciences of Ukraine*, **11**, 71–75 [in Russian].
27. Cressault, Y., Murphy, A.B., Teulet, Ph. et al. (2013) Thermal plasma properties for Ar–Cu, Ar–Fe and Ar–Al mixtures used in welding plasma processes: II. Transport coefficients at atmospheric pressure. *J. Phys. D: Appl. Phys*., **46**, 415207. DOI: https://doi.org/10.1088/0022-3727/46/41/415207
28. Essoltani, A., Proulx, P., Boulos, M.I. et al. (1994) Volumetric emission of argon plasmas in the presence of vapours of Fe, Si and Al. *Plasma Chem. and Plasma Proc*., 14(**4**), 437–450. DOI: https://doi.org/10.1007/BF01570206
29. Demchenko, V.F., Krivtsun, I.V., Krikent, I.V., Shuba, I.V. (2017) Force interaction of arc current with self-magnetic field. *The Paton Welding J.*, **3**, 15–24. DOI: https://doi.org/10.15407/tpwj2017.03.03

ORCID

I.V. Krivtsun: 0000-0001-9818-3383,
I.V. Krikent: 0000-0002-4196-6800

CONFLICT OF INTEREST

The Authors declare no conflict of interest

CORRESPONDING AUTHOR

I.V. Krivtsun
E.O. Paton Electric Welding Institute of the NASU
11 Kazymyr Malevych Str., 03150, Kyiv, Ukraine.
E-mail: krivtsun@paton.kiev.ua

SUGGESTED CITATION

I.V. Krivtsun, I.V. Krikent, V.F. Demchenko (2023) Influence of weld pool surface depression on burning conditions of an arc with a refractory cathode. *The Paton Welding J.*, **8**, 44–49.

JOURNAL HOME PAGE

https://patonpublishinghouse.com/eng/journals/tpwj

Received: 24.06.2023
Accepted: 07.08.2023